Sonic wave velocity and X-ray tomography images for partially saturated rocks. Evidence of microscopic fluid distribution effect on acoustic properties.

Thierry Cadoret (*,**), **Dominique Marion** (**) & **Bernard Zinszner** (*)

** Elf Aquitaine Company

* Institut Francais du Pétrole

Abstract Elastic waves velocities were measured in the laboratory on partially water-saturated limestones using large (1 meter length) and homogeneous resonant bars.

We used two different saturation methods: 1/ Drying, which is a drainage process. 2/ Spontaneous imbibition followed by progressive depressurization in order to increase water saturation (S_w).

In both cases, shear velocity (V_S) is not dependent on saturating method whereas compressional velocity (V_P) shows a clear dependence on it. This is observed at high levels of saturation where V_P exhibits a large increase with increasing S_w in the drying experiment. In contrast, V_P remains relatively constant with increasing S_w using the depressurization method.

To study the fluid distribution in the samples, we performed X-ray tomography at different values of S_w for both saturation methods. Images of depressurized samples show a great homogeneity of saturation at the millimetric scale at all saturations. In the drying experiment, X-ray images at high water saturation levels reveal heterogeneous saturation in the form of centimetric clusters.

From these experimental results, we conclude that the discrepancy between P-wave velocity during drainage and imbibition is related to clear differences in fluid repartition.

INTRODUCTION

Since the pioneering works of Wyllie, Gregory and Gardner (L.W. and G.H.F.) in 1956 and 1958, the dependence of acoustic wave velocities on gas saturation has been widely studied in the laboratory.

In the ultrasonic (0.5 MHz and above) frequency range the velocity (V) vs. water saturation (Sw) relationship seems rather complex, depending strongly on rock type and porosity (Gregory 1976, for instance). This confusing behavior is sometimes related to rock heterogeneity at the ultrasonic wavelength scale (Lucet and Zinszner 1992). Indeed, in the sonic frequency band (1 to 10 kHz), V vs. S_w plots are easier to explain (Murphy 1984), but published experimental results are scarce.

Moreover, V vs. S_w relationship could depend on the method used to reach a given saturation, (Domenico 1977, Knight and Nolen-Hoeksema 1990). These authors studied the influence of fluid distribution on acoustic velocity in the ultrasonic frequency band. In this case, the characteristic wavelength is millimetric and approaches the pore scale. Our goal is to investigate this problem in the sonic frequency range (i.e. metric wavelength and decimetric characteristic length for fluid distribution inhomogeneity). Experiments with metric wavelength present several advantages: 1) one can avoid most of the heterogeneity induced by the rock fabric (grain scale), 2) laboratory frequencies are identical to the ones used in the field for acoustic logging, 3) one can use X-ray tomography technique to monitor the fluid repartitions in the sample at a scale much smaller (millimetric) than the acoustic wavelength and 4) with the use of large (1 m) samples, we minimize the edge effects in the saturation processes.

SATURATION METHODS

In order to reach different fluid distributions for a given value of S_w, we used different saturation methods. The two types of saturation processes used in the laboratory are : drainage when S_w decreases, imbibition when S_w increases (with water as the wetting fluid). Having choosen the saturation techniques, we have to take into account some particularities of our experiment: unusually large sample, drastic restriction on rod jacketting for acoustic measurement, etc... We selected the two following

methods which were validated a posteriori by X-ray tomography saturation maps:

Drainage by Air/Brine Drying

It is well known (see Dullien 1979, for a review) that, at the beginning of a drying experiment, the water-loss per unit of time, is proportional only to the sample surface area in contact with the gas and to the thermodynamic state of this gas and does not depend to the petrophysical characteristics of the rock. During this phase, the displacement of fluids inside the porous network allows a quasi-instantaneous equilibriumof the capillary pressure through the whole sample. This mechanism, which appeared to be verified for S_w higher than 20% for most of our samples and our laboratory conditions, can be considered as a true drainage process. It was particularly well suited to our resonant bar experiment.

Pseudo-imbibition by Depressurization

A progressive and controlled imbibition is not as easy to perform than drying. To approach this saturation mechanism, we used the depressurization technique. The dry sample was first put in contact with water to allow a spontaneous imbibition. The sample reached then a S_w value that is a petrophysical characteristic of the rock (sometimes called Hirschwald coefficient). Then, to reach higher S_w values, the sample was immersed in a water tank and the pressure of the water was decreased in order to release a fraction of the air previously trapped in the porous media. Finally, a new imbibition is started by re-equilibrating the water to the atmospheric pressure.

Repeating this process, we could achieve controlled partial saturation between the value of S_w corresponding to spontaneous imbibition and a maximum S_w which depends on the smaller pore access radii. For very permeable rocks, the maximum S_w is very close to 100%. Using CO_2 gas (highly soluble in water) instead of air, one can achieve S_w=100% even for less permeable rocks. Finally we have to remind that even with the air/water couple of fluids, depressurization is not a pure imbibition process.

ACOUSTIC MEASUREMENTS

Resonant Bar Technique

The laboratory technique used to measure acoustic properties of rocks in the sonic (kilohertzian) frequency range is the resonant bar (Birch and Bancroft, 1938; Winkler, 1979; Lucet et al., 1991).

It consists in vibrating a rod of material with variable frequency stress to generate standing waves in it. The rod is held in its center. In the experiments reported here, rods are typically 110 cm in length and 8 cm in diameter (fig. 1). Stress is applied at one end of the rod through magnets (attached to the bar) wich are excited by coils, driven with variable frequency. Vibrations amplitudes are measured at the other end with an accelerometer and are recorded on a X-Y plotter as a function of the frequency.

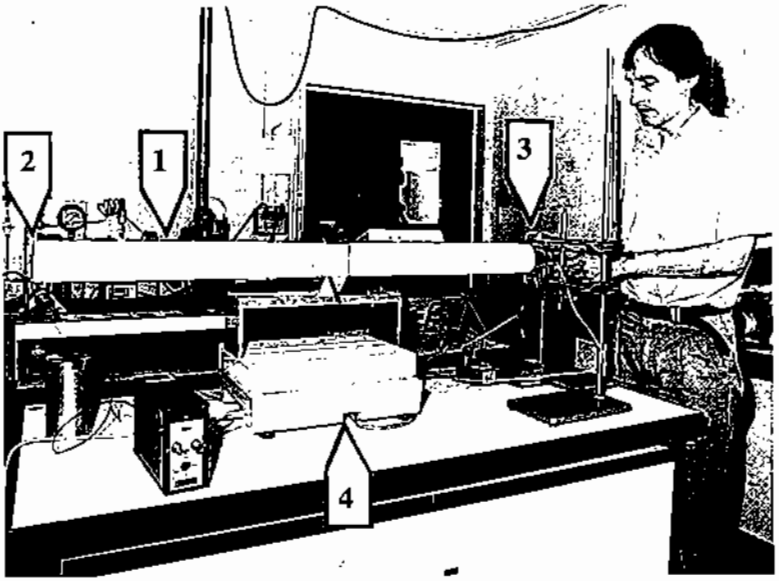

FIGURE 1 : Resonant Bar experimental set-up.
1/ Limestone rod.
2/ Accelerometer.
3/ Excitating coils.
4/ Scales for saturation monitoring.

Velocities are calculated from the resonant frequencies: resonance occurs when the length of the rod is half a multiple n of the wavelength l :

$$l = \frac{n\lambda}{2} \qquad (1)$$

Velocity can then be written as:

$$V = \frac{2clf}{n} \qquad (2)$$

where c is a correction factor (very close 1 in our experiments) and f is the resonant frequency.

Two modes of vibrations were used: the extensional mode and the torsional mode. The first one leads to the measurement of extensional velocity V_e (related to the Young's modulus). The torsional mode allows the measurement of shear velocity V_s (related to the shear modulus).

From these two velocities, the compressional velocity V_p can be computed:

$$V_p^2 = \frac{V_s^2(4V_s^2 - V_e^2)}{3V_s^2 - V_e^2} \qquad (3)$$

When dealing with large, cylindrical, homogeneous bar, this resonating system is very accurate (better than 2%). This accuracy was checked by measuring artificial material (plastic, glass etc.). To verify the reproducibility of the experiment, we performed two de-saturations in the same conditions. The results is shown on fig. 2c. Sw is known by weight of the sample during the experiment. The error on this value is lower than 1%.

Experimental Results

One of the main factors affecting acoustic wave velocities in rocks is the effective pressure imposed on the sample (see Bourbie et al. 1987, for a review). We want to perfom resonant bar experiments in room conditions and minimize any pressure effects on V vs. S_w results. Thus we have to select rocks which are fairly porous and exhibit little sensitivity to effective pressure as well. We chose 8 kinds of quarry limestones with porosity ranging from

18 % and 40% and permeability ranging from 8 mD to 4000 mD. In the acoustic results presented thereafter, we do not deal with the velocities at very low water saturation (S_w < 10%). We did not study this particular saturation state (where water adsorbtion plays a major role) for two reasons: 1/ in our experiments, we could reach this saturation with only one technique (drying), 2/ X-ray tomography have shown that the saturation distribution was strongly dependent on the shape of the sample (radial zonation).

Shear wave velocities

For the 8 samples considered, the relationship between shear wave velocity (V_s) and S_w is simple: V_s decreases regularly with increasing S_w and is clearly non dependent on the saturation method (Fig 2a and 2b). These results confirm the well established opinion that the rock shear modulus m is non dependent on fluid content (either fluids nature or saturation). Recalling the formula:

$$V_S = \sqrt{\frac{m}{r}} \qquad (4)$$

we see that the sligth variation of V_s with S_w is directly related to the variation in rock density (r) when water saturation is changing.

Compressional wave velocities

The situation is quite different when dealing with compressional wave velocities (V_p). Only one sample (Saint Pantaleon Limestone Fig. 2a) exhibits a V_p vs. S_w relationship similar to the V_s plots (density effect only, and no dependence on saturation method). We have presently no explanation for this unusual behavior carefully checked.

All the other samples show the same trend, summarized on the Estaillades limestone plot (Fig 2b, enlarged Fig.2c):

- for S_w lower than approximately 80%, drying and depressurization give the same V_p value and the continuous decrease of V_p with increasing S_w is perfectly explained by the density effect, as seen for shear wave.
- for higher S_w, drying and depressurization do not lead to the same velocity values any more. V_p exhibits a large increase with increasing S_w, in the drying experiment. With the depressurization method the increase in V_p can only be observed close to the total water saturation.

We will see in the next paragraph that great differences in fluid repartitions explain this situation.

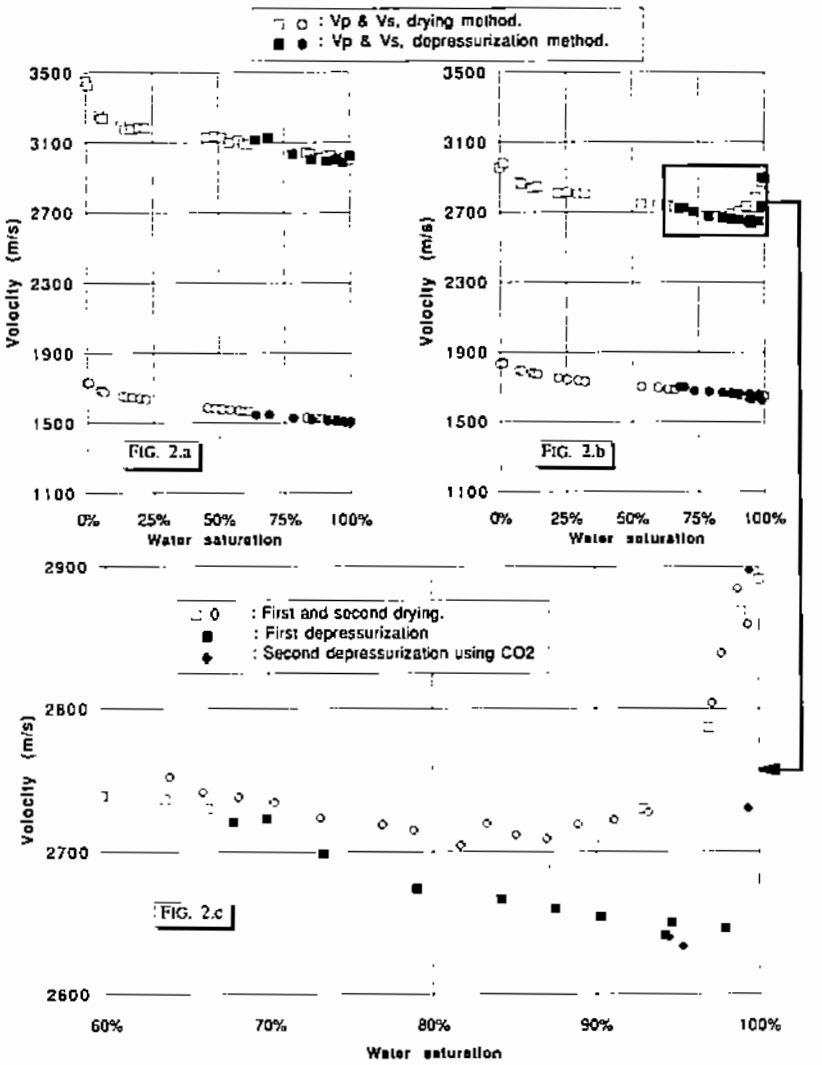

FIGURE 2 : velocity *vs.* water saturation with different methods of saturation.

a/ Saint-Pantaleon limestone (Φ=35%, K=4000 mD).

b/ Estaillades limestone (Φ=30%, K=260 mD). This V_p behaviour is representative of 7 samples on the 8 limestone.

c/ Enlarged view of V_p *vs.* S_w for Estaillades limestone.

SATURATION MAPPING USING X-RAY TOMOGRAPHY

X-ray Tomography Technique

Principle of X-ray tomography experiments

We use X-ray tomography imaging to visualize the porosity distribution in the limestones and the fluid repartition at various level of water saturation. This method (Wellington & Vinegar, 1985) gives an image of the radiologic density distribution in a 3 mm thick rock slice. X-rays propagate through the sample and then, are collected with a set of receivers disposed in a circular arc. By rotating the emitter/receiver system around the sample, it is possible to record numerous ray paths. This data is transmitted to a computer that calculates an image in terms of the product of density (r) and X-ray absorption (a) of the medium, where a depends on the mineral and X-ray energy. Thus, each tomography is a digital picture composed by an array of digits corresponding to the a*r product. The samples used are 20 cm long cylindrical rods with a diameter of 8 cm (same diameter as the resonant bar), cut adjacent to the resonant bar.

Computing of the saturation maps

Figure 3 presents the different mathematical steps we performed to obtain the gas saturation maps.
Three X-ray tomography of the same slice of the sample at different saturation states are necessary for each gas saturation maps. The porosity map is given by substraction of the fully water saturated rock image by the dry rock image. Substraction of the image of a rock at a given fluid saturation by the picture of the fully water saturated sample gives an image in terms of gas content. The division of this image by the porosity map gives finally the gas saturation map.

These arithmetic calculations between images require a perfect reproducibility in the positionning of the sample. To achieve this, each sample is mounted on an aluminium plate which can be precisely placed on the X-ray tomography acquisition bed.

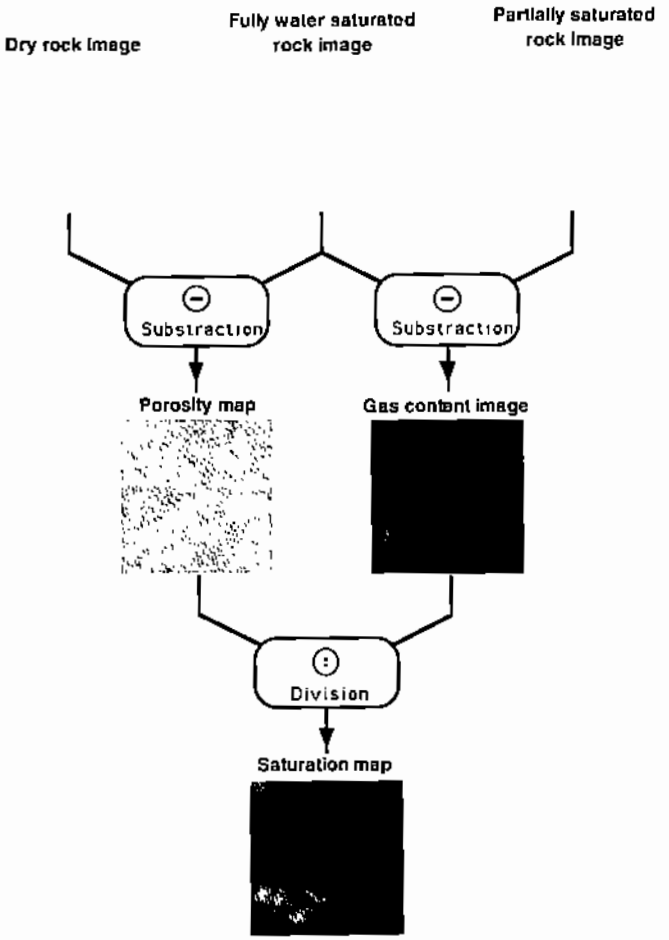

FIGURE 3 : Flowchart of the different steps of saturation map elaboration. The images used correspond to Brauvilliers limestone.

Reliability of the Results

Definition of the noise on the images

Figure 4.a shows a typical example of saturation maps during drying experiment. The white parts correspond to gas-bearing zones. The rest can be viewed as fully water saturated zones. Nevertheless these zones does not appear as plain colour but rather as speckled area. These closely mixed colours are not a sign of variation in the fluid saturation. They must be considered as an experimental noise which have several origins. First, it exists an incertainty directly caused by the X-ray tomography method which has a limited resolution. Typically, in the case of this study, the resolution of the tomography is limited to a volume of 0.2*0.2 mm wide and 3 mm thick. Furthermore, the necessity to move the sample between each measurement induces an imperfect reproducibility in the positionning of the sample.

FIG. 4.a

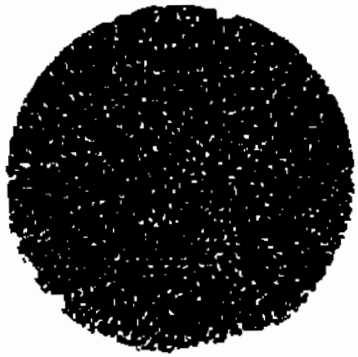

FIG. 4.b

FIGURE 4 : Saturation maps of Brauvilliers limestone. White area correspond to gas bearing zones. a/ Saturation obtained by drying. Sw=92%
b/ Fully water saturated sample.

To illustrate this definition of the noise, we have computed a gas saturation map for a fully water saturated sample (image 4.b). This image exhibits only the noise. We see that it presents the same aspect as the darker zones of image 4.a. By image

processing, it is possible to remove this noise without distorting the fluid saturation patterns.

Accuracy of X-ray tomography fluid saturation and porosity values

We have checked that the level of fluid saturation given by the saturation maps matches closely the values obtained by weight. The saturation value given by X-ray tomography is known with an uncertainty of 2% of saturation. The porosity has been checked too. Here again, we find approximately the same values by porosimetry and by integration of the porosity map. The error on porosity value computed from images is 1%.

Representativity of the results obtained on each slices

We have checked that for a given fluid saturation, the average value of saturation obtained with the saturation maps does not vary significantly from one slice to another. So, it is reasonable to assume that the observation on one slice is fairly representative of the global state of the rock. Furthermore, this is a supporting evidence of the homogeneity of the limestones we selected.

Reproducibility of the drying patterns

The figures 6.a and 6.b show the same slice of rock at approximately the same fluid saturation obtained by two distinct drying experiments. These pictures reveal the same patterns of gas bearing zones invading the saturated sample. This shows the reproducibility of the saturation maps obtained with the drying technique.

Isotropy of fluid distribution pattern

In order to visualize the fluid distribution in axial planes (perpendicular to the plane where the slices are recorded), we performed a reconstruction of the saturation map in various longitudinal planes by interpolating closely spaced slices. Figures 5.a and 5.b show the result of this reconstruction for a drying sample at two different levels of saturation.

FIG. 5.a

FIG. 5.b

Orientation of the sample for X-ray tomography imagery :

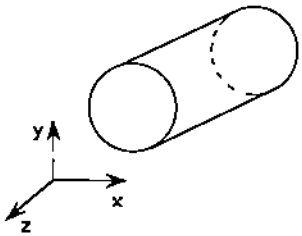

FIGURE 5 : Reconstructed saturation map of Estaillades limestone. This image of the x.z plane are obtained by interpolation of the tomography recorded in the x.y plane. White patterns correspond to gas bearing zones.
a/ Drying experiment, Sw=94%.
b/ Drying experiment, Sw=92%.

It must be emphasized that this interpolation tends to magnify the size of the patterns parallel to the reconstruction plane. This artefact explains partly the streched aspect of the gas bearing zones. The fluid repartition on this two images does not seem to reveal a particular continuity of the fluid distribution in the reconstruction axis. It is interesting to compare figure 6.c and figure 5.b which correspond to close saturation state in two perpendicular planes. It shows that the size of the gas bearing zones are quite similar. Thus, no anisotropy in the fluid distribution patterns can be noticed.

Results and Conclusion Obtained from the X-ray Tomography

Reliability of drying and depressurization as saturation methods

X-ray tomography comforts the validity of drying and depressurization as fluid saturation methods. Depressurization allows to obtain very homogeneous saturations at the millimetric scale even for very high water saturation. The bench top drying can also give an homogeneous fluid saturation. But this homogeneity is only obtained at the centimetric scale for high Sw (S_w>80%). It must be emphasized that even for high water saturation (S_w=92%), the geometry of the sample does not interfere with the fluid distribution patterns. It is only when we consider extreme saturation (S_w<15% or S_w>95%) that clear heterogeneity in the fluid distribution can be linked to the geometry of the sample. In between these two limits the saturation patterns resulting from the drying process appear to be only controled by the intrinsec properties of the rock.

Clear difference in fluid repartition between drying and depressurization

We have to emphasize the fact that the saturation maps recorded on Estaillades limestone and shown on figure 6 are representative of all our set of samples. One of the most interesting feature pointed out by this study is the clear difference of fluid distribution between the saturations obtained by depressurization or by drying as shown on figure 6.c and 6.d. These figures correspond to the same slice at very close water saturation.

At this point, it is important to recall that a petrophysical property (in our case the gas saturation value) must be considered as the averaged value of an elementary unit of volume (elementary cell). Figures 6.a or 6.c, show images of drying rocks that feature centimetric clusters of gas bearing pores. Thus, in this case, it is only when considering centimetric elementary cell that the saturation is homogeneous. On the other hand, Figure 6.d shows the fluid distribution given by depressurization. The resolution of X-ray tomography imaging does not permit to know exactly the size of the elementery cell in this case. However, saturation can be considered as homogeneous at the millimetric scale

FIG 6.a : Drying, Sw=95%

FIG 6.b : Drying, Sw=96%

FIG 6.c : Drying, Sw=92%

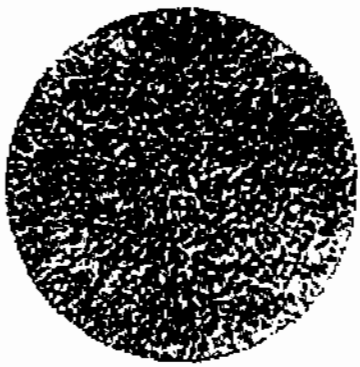

FIG 6.d : Depressurization, Sw=92%

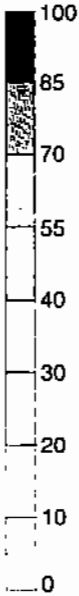

Water saturation scale (%)

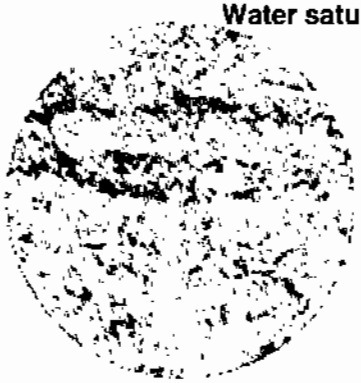

FIG 6.e : Drying, Sw=61%

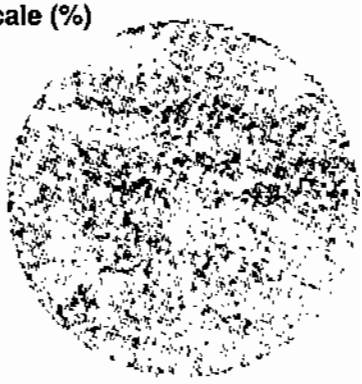

FIG 6.f : Depressurization, Sw=69%

Figure 6 : Saturation maps - Estaillades limestone.

For S_w<80%, difference of fluid repartition between saturation obtained by drying or by depressurization vanishes (see figure 6.e and 6.f). In both cases the saturation is homogeneous at the millimetric scale.

INFLUENCE OF FLUID DISTRIBUTION ON ACOUSTIC VELOCITY

Having shown that the V_s versus Sw behaviour is independent on the saturation method for all the samples, we will concentrate this discussion on the V_p vs. S_w results compared to the fluid distribution observed by X-ray tomography.

The acoustic results show that for S_w ranging approximately between 15% and 80%, V_p is independant of the saturation method. In this range of saturation, it appears on saturation maps that S_w is homogeneous at the pore scale. When considering S_w higher than 80%, V_p shows two distinct behaviors. With the depressurization method, the compressional velocity tends to follow a curve governed by the density effect until S_w is very close to total water saturation. X-ray tomography reveals that this saturation technique induces a fluid saturation homogeneous at the millimetric scale even for very high S_w. For fluid saturation obtained by drying, V_p increases smoothly towards the fully water saturated value. In the same time, the fluid distribution is homogeneous only at the centimetric scale. Fully water saturated area of centimetric dimensions coexists with partially saturated patterns.

Pure water exhibits a much lower compressibility than air/water mixture even for low air proportion. The existence of large enough, fully water saturated area explains the rock stiffening and the early increase of V_p for higher S_w. These fully water saturated areas increase the effective modulus of the rock without modifying the homogeneity at the wavelength scale.

On the other hand, when the rock is saturated using the depressurization method, the homogeneous distribution of gas bubbles at the pore scale prevent any stiffening of the rock but for S_w very close to 100%.

CONCLUSIONS

Our experimental results lead to two main conclusions:

- X-ray tomography validates the saturation methods we used in the experiments. Drying is an easy and convenient way to perform air/water drainage upon a large range of saturation (15% < S_w <95% ?). Depressurization gives air/water distributions very homogeneous at the microscopic (pore) scale, even in the case when S_w tends towards 100%.

- For higher water saturation, sonic P-wave velocities depend clearly on the saturation method. X- ray tomography saturation maps allow to relate these velocity differences to marked differences in the saturation geometry (variation of the scale of homogeneization). This observation emphasizes the necessity of a careful approach in interpretating elastic wave velocity in term of fluid saturation when the microscopic fluid distribution in the porous media is not perfectly known.

This study shows that Vp vs. S_w data contain informations on fluid saturation and fluid distribution. Thus, to interpret these data in terms of one of this factor, we have to be sure that the other parameter is known.

Acknowledgments

This research was done at the Institut Français du Pétrole Rock Physics Laboratory with financial support from Elf-Aquitaine Co. We wish to thank M.T. Bieber, the IFP X-Ray lab and M. Masson for their help in experiments.

REFERENCES

Birch, F., and Bancroft D. (1938) Elasticity and internal friction in a long column of granite. *Bull. Seis. Soc. Am*, 38, pp. 243-254

Bourbié,T., et al. (1987) *Acoustics of porous media*. Gulf Publishing Co., Houston

Domenico, S.N. (1977) Elastic properties of unconsolidated porous sand reservoir. *Geophysics*, 42, pp. 1339-1368

Dullien, F.A.L. (1979) *Porous media: fluid transport and pore structure*. Academic Press, New York

Gregory, A.R. (1976) Fluid saturation effects on dynamic elastic properties of sedimentary rocks. *Geophysics* , 41, pp. 895-921

Knight, R. and Nolen-Hoeksema R. (1990) A laboratory study of the dependence of elastic wave velocities on pore scale fluid distribution. *Geophy. Res. Letters*, 17, N°10, pp. 1529-1532

Lucet N., Rasolofosaon, P.N.J., Zinszner, B. (1991) Sonic properties of rocks under confining pressure using the resonant bar technique. *J. Acoust. Soc. Am.*, 89, N° 3, pp. 980-990

Lucet N., Zinszner B. (1992) Effects of heterogeneities and anisotropy on sonic and ultrasonic attenuation in rocks. *Geophysics*, 57, N° 8

Murphy W.F.III (1984) Acoustic measures of partial gas saturation in tight sandstones. *Jour. of Geophys. Res.*, 89, N° B13, pp. 11549-11559

Wellington, S.L.,Vinegar, H.J. (1985) CT studies of surfactant induced CO2 mobility control *S.P.E.* paper N° 14393 (Las Vegas Meeting)

Winkler K. (1979) The effects of pore fluids and frictional sliding on seismic attenuation. *Ph.D Thesis*, Stanford, USA

Wyllie, M.R.J., Gregory, A.R., Gardner, L.W. (1956) Elastic wave velocities in heterogeneous and porous media. *Geophysics*, 21, pp. 41-70

Wyllie M.R.J., Gregory A.R., Gardner G.H.F. (1958) An experimental investigation of factors affecting elastic wave velocities in porous media. *Geophysics*, 23, pp. 459-49